LBNL-42717
Preprint

ERNEST ORLANDO LAWRENCE
BERKELEY NATIONAL LABORATORY

Lysozyme Net Charge and Ion Binding in Concentrated Aqueous Electrolyte Solutions

Daniel E. Kuehner, Jan Engmann,
Florian Fergg, Meredith Wernick,
Harvey W. Blanch, and John M. Prausnitz

Chemical Sciences Division

January 1999

Submitted to
The Journal of Physical Chemistry

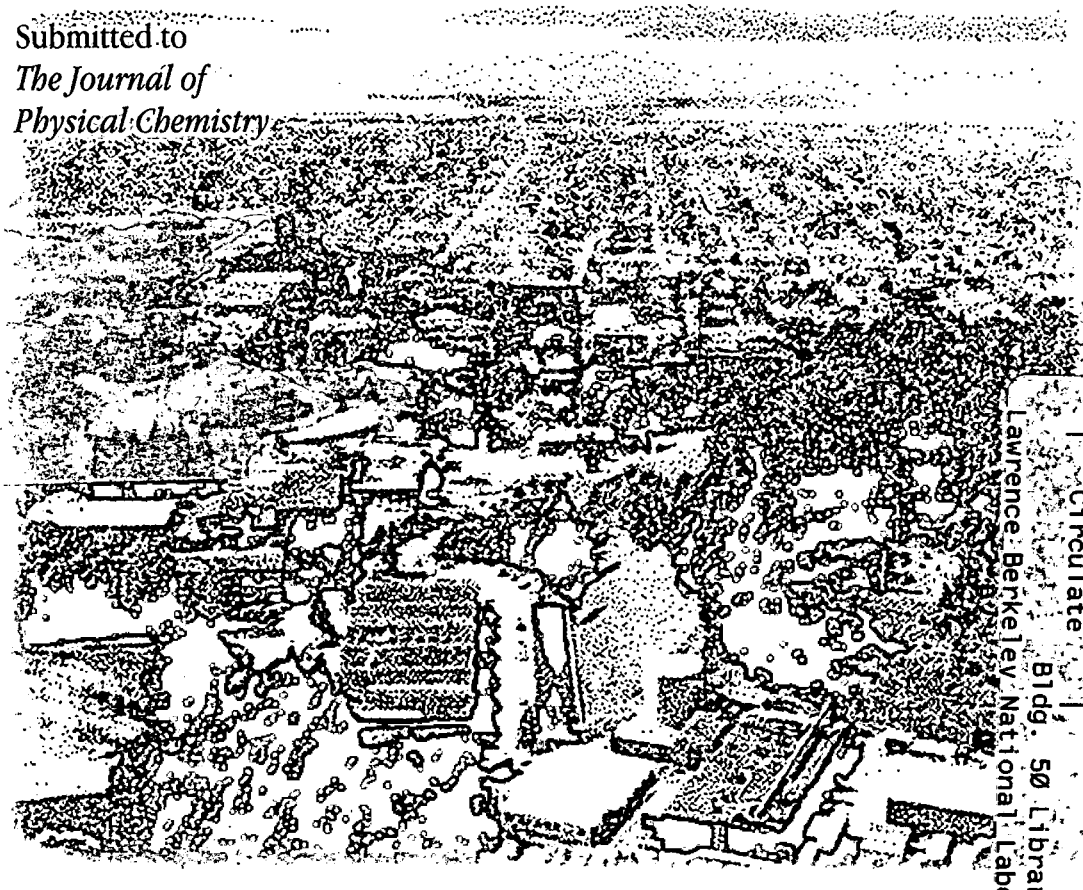

DISCLAIMER

LBNL-42717

Lysozyme Net Charge and Ion Binding in Concentrated Aqueous Electrolyte Solutions

Daniel E. Kuehner, Jan Engmann, Florian Fergg,
Meredith Wernick, Harvey W. Blanch and John M. Prausnitz
Department of Chemical Engineering
University of California
and
Chemical Sciences Division
Lawrence Berkeley National Laboratory
University of California
Berkeley, CA 94720, U.S.A.

January 1999

This work was supported by the Director, Office of Energy Research, Office of Basic Energy Sciences, Chemical Sciences Division of the U.S. Department of Energy under Contract Number DE-AC03-76SF00098.

Lysozyme Net Charge and Ion Binding in Concentrated Aqueous Electrolyte Solutions

Daniel E. Kuehner[1], Jan Engmann[2], Florian Fergg[3], Meredith Wernick, Harvey W. Blanch[†] and John M. Prausnitz[†,‡,*]

[†]Department of Chemical Engineering, University of California, Berkeley, CA 94720

and

[‡]Chemical Sciences Division, Lawrence Berkeley National Laboratory, Berkeley, CA 94720

ABSTRACT

Hydrogen-ion titrations were conducted for hen-egg-white lysozyme in solutions of potassium chloride, over the range of pH 2.5 - 11.5 and for ionic strengths to 2.0 M. The dependence of lysozyme's net proton charge, z_p, on pH and ionic-strength in potassium-chloride solution is measured. From the ionic-strength dependence of z_p, interactions of lysozyme with potassium and chloride ions are calculated using the molecular-thermodynamic theory of Fraaije and Lyklema[1]. Lysozyme interacts preferentially with up to 12 chloride ions at pH 2.5. The observed dependence of ion-protein interactions on pH and ionic strength is explained in terms of electric-double-layer theory. New experimental pK_a data are reported for eleven amino acids in potassium-chloride solutions of ionic strength to 3.0 M.

[1] Present address: Bristol-Myers Squibb Pharmaceutical Research Institute, 1 Squibb Drive, P.O. Box 191, North Brunswick, NJ 08903-0191; email: Daniel_E._Kuehner@ccmail.bms.com

[2] Present address: Department of Chemical Engineering, University of Cambridge, Pembroke Street, Cambridge CB2 3RA, UK; email: je224@hermes.cam.ac.uk

[3] Present address: Department of Chemical Engineering, Technical University of Hamburg-Harburg, Eissendorfer Strasse 38, D-21071 Hamburg, Germany; email: fergg@tu-harburg.de

* Author to whom correspondence should be addressed

1. INTRODUCTION

Salt ions play an important role in protein-protein interactions in aqueous solutions at all ionic strengths. At low salt concentrations, ions stabilize proteins in solution *via* reduction of electrostatic repulsion between charged protein macromolecules (*i.e.*, the salting-in effect). As the salt concentration increases, repulsive electrostatic interactions are further screened; other protein-protein forces (notably attractive Hamaker dispersion forces) can then operate toward aggregation and precipitation. At higher salt concentrations, preferential hydration of salt ions can desolvate proteins, causing them to aggregate, precipitate, or crystallize (the salting-out effect). Molecular-thermodynamic models describing protein phase separation in concentrated aqueous salt solutions require physicochemical information about the interactions between protein molecules and salt ions. For example, models based on potential-of-mean-force descriptions of interactions in solution require information for ion-protein as well as protein-protein interactions[2-6].

This work explores the dependence of hen-egg-white lysozyme's net charge, z_p, and interaction with chloride and potassium ions, on solution pH and ionic strength using experimental results from hydrogen-ion titrations. Hydrogen-ion titrations have been conducted in potassium-chloride solutions for lysozyme and eleven amino acids, over a broad range of ionic strength and pH. From the ionic-strength dependence of the protein titration curves, ion-binding numbers have been calculated using a molecular-thermodynamic model derived by Fraaije and coworkers[1,7,8] and are reported here. Discussion is presented on the effect of solution ionic strength on the surface charge of lysozyme, on pK_a values of the various titratable groups, and on the protein titration curve.

2. HYDROGEN-ION TITRATIONS OF PROTEINS

In a protein molecule, hydrogen ions bind covalently to the side chains of acidic and basic amino-

acid residues and at the amino and carboxyl termini of the amino-acid chain(s) of the protein. At any given pH, the protonation state of each titratable group depends on its hydrogen-ion dissociation constant, or K_a. If the values of the individual K_as of all the titratable groups are known, the net proton charge of the protein, z_p, may be calculated as a function of pH as follows. The hydrogen-ion-dissociation equilibrium constant of site i, $K_{a,i}$, is given by:

$$K_{a,i} = \frac{a_{H^+} \cdot a_{A_i}}{a_{HA_i}} \tag{1}$$

where a stands for activity. The hydrogen-ion activity is given by $a_{H^+} = c_{H^+}\gamma_{H^+}$, where c_{H^+} and γ_{H^+} are the molar concentration and the ionic-strength-dependent activity coefficient of the hydrogen ion, respectively; and the activities of the protonated and deprotonated states are given by $a_{HA_i} = c_{HA_i}\gamma_{HA_i}$ and $a_{A_i} = c_{A_i}\gamma_{A_i}$, respectively. The logarithm of equation (1) yields:

$$\mathrm{p^oH} - \mathrm{p^o}K_{a,i} = \log\left(\frac{c_{A_i}}{c_{HA_i}}\right) \tag{2}$$

where the concentration-based definitions $\mathrm{p^oH} \equiv -\log c_{H^+}$ and $\mathrm{p^o}K_{a,i} \equiv -\log(c_{H^+}c_{A_i}/c_{HA_i})$ are introduced. These are related to the conventional activity-based definitions $\mathrm{pH} \equiv -\log a_{H^+}$ and $\mathrm{p}K_{a,i} \equiv -\log K_{a,i}$ through the activity coefficients:

$$\mathrm{p^oH} = \mathrm{pH} + \log\gamma_{H^+} \tag{3a}$$

$$\mathrm{p^o}K_{a,i} = \mathrm{p}K_{a,i} + \log(\gamma_{H^+}\gamma_{A_i}/\gamma_{HA_i}) \tag{3b}$$

From equations (1) and (2), the net protein charge, z_p, is calculated as a function of pH. The net charge of the protein molecule also depends on the ionic strength of the solution. Addition of salt attenuates electrostatic interactions in the local micro-environment of each titratable group, altering the activity coefficients of the protonated and deprotonated states and thereby shifting the pK_a of that group. Since proteins are in essence large, conformationally-complex polyelectrolytes, experimental determination of the activity coefficients of individual titratable groups as a function of solution chemistry is difficult and has only recently become possible *via* NMR[9,10].

With the advent of powerful computational tools, many efforts have been made to calculate *à priori* the pK_as of titratable side-chains in hen-egg-white lysozyme and other well-studied proteins[11-16]. In general, these methods describe the titration equilibrium for a given site as:

$$pK_a = pK_{a,\text{model}} + \Delta pK_a \qquad (4)$$

where $pK_{a,\text{model}}$ refers to a hypothetical case wherein the titrating group has no intramolecular electrostatic interactions with the rest of the protein. Approximate values of $pK_{a,\text{model}}$ may be obtained experimentally from titration of fully denatured proteins or end-blocked polypeptides containing the side-chain of interest. The perturbation, ΔpK_a, contains all the electrostatic effects introduced by placing the titrating side-chain in the environment of a native protein molecule. In an early computational study, Bashford and Karplus[12] calculated pK_as for titratable groups in lysozyme at ionic strength 0.1 M; using crystallographic data to define lysozyme's shape and finite-difference methods to solve the linearized Poisson-Boltzmann equation for the electrostatic-potential profile around the molecule; pK_as are shown in Table 1. This method assumes the

protein structure to be rigid in its crystallographic shape. However, it has been recognized that the lack of conformational mobility of the side chains leads to overestimation of electrostatic pK_a perturbations. The physical rationale is as follows: when titration brings a residue into the charged state, the surrounding environment (solvent and protein) reorients in an effort to offset the charge, reducing the magnitude of the pK_a perturbation. Beroza and Case[14] incorporated side-chain flexibility, using conformational sampling methods; see Table 1. Table 1 also lists "experimental" pK_as regressed by Kuramitsu and Hamaguchi[17] from lysozyme titration curves measured in 0.1 M potassium-chloride solutions. The computed pK_as of Beroza and Case show closer agreement, on average, with experiment than those of Bashford and Karplus.

A conclusive example of the power of these models to describe the electrostatic environment around the protein is given by Glu-35 in lysozyme's active site. The experimentally observed value of the pK_a of Glu-35, 6.1, is abnormally high[9,17]; for free glutamic acid, the side-chain pK_a = 4.2. The deprotonated state of Glu-35 has a strong interaction with the negative charge of nearby Asp-52 and with the negative end of the macrodipole created by the α-helical conformation of residues 25-35[11]. These repulsive electrostatic interactions favor the protonated state of Glu-35, resulting in a large positive pK_a perturbation. Effects such as these cannot be described *à priori* with empirical models.

3. TITRATION EXPERIMENTS

In a pH measurement, the measured electrode voltage, E, and the hydrogen-ion activity, a_{H^+}, are related by a Nernst-type equation:

$$E = E^{ref} + S \cdot \log a_{H^+}$$
$$= E^{ref} - S \cdot [\mathrm{p^oH} - \log \gamma_{H^+}] \qquad (5)$$

where E^{ref} is the electrode standard potential and S is a slope, determined by an electrode-calibration titration prior to each protein titration. The hydrogen-ion activity coefficient was calculated using Pitzer's model for multicomponent electrolyte solutions[18]; γ_{H^+} varied with ionic strength but was independent of hydrogen-ion concentration over the range $2 < \mathrm{pH} < 12$.

3.1. Electrode-Calibration Titration

Calibration titrations were performed by serial addition of aliquots of an alkaline titrant solution containing 0.1 M KOH to a potassium-chloride solution ("blank") previously acidified with HCl to approximately pH 2.5. The blank and the titrant solutions had the same total ionic strength. Aliquots of the alkaline titrant solution were added until the solution pH reached approximately 11.5, yielding data in the form $\{E, V^{added}\}$. Mass balances for hydrogen and hydroxide ions enabled calculation of p°H (*via* the water dissociation reaction) and the electrode slope and intercept. Values of E^{ref} and S obtained for each electrode calibration were considered valid for one day at most. Separate calibration titrations were performed for each protein or amino-acid titration, which were carried out immediately following the calibration titrations.

3.2. Protein and Amino-Acid Titrations

For titration solutions containing protein or amino acid, a modified set of mass balances accounted for the reaction of hydrogen ion with the protein or amino acid. With these mass balances and the electrode slope and intercept obtained from the calibration titration, the change in charge of the

protein or amino acid with p°H was calculated. All titration curves reported here are referenced to the isoelectric point (where $z_p = 0$) of lysozyme, p°I = 11.16. The concentration-based isoelectric point, p°I, is given by p°I = pI + $\log \gamma_{H^+}$ and was assumed not to vary with ionic strength, as discussed below.

3.3. Materials

Hen-egg-white lysozyme (M = 14,500 g/mol) was obtained from Sigma Chemical Company, St. Louis, MO (L-2879; CAS# 9066-59-5; grade VI: chloride, 3x crystallized). The following L-amino acids were obtained from Sigma and were used without further purification: alanine (A-5824; CAS# 56-41-7), arginine (A-5006; CAS# 74-79-3; free base), asparagine (A-8824; CAS# 5794-13-8; monohydrate), aspartic acid (A-8949; CAS# 56-84-8; free acid), cysteine (C-7755; CAS# 52-90-4; free base), glutamic acid (G-6904; CAS# 56-86-0; free acid), histidine (H-8776; CAS# 71-00-1; free base), isoleucine (I-7268; CAS# 73-32-5), leucine (L-5652; CAS# 61-90-5), lysine (L-5501; CAS# 56-87-1; free base), and tyrosine (T-8909; CAS# 60-18-4; free base). Potassium hydrogen phthalate (CAS# 877-24-7) was obtained from Aldrich Chemical Company, oven dried and stored under vacuum. Standardized stock solutions of hydrochloric acid (CAS# 7647-01-0) and potassium hydroxide (CAS# 1310-58-3) of concentration 0.995 - 1.005 N were purchased from Fisher Scientific, along with crystalline potassium chloride (CAS# 7447-40-7; ACS grade). Distilled, deionized and degassed water was used to make all solutions.

Protein solutions were prepared by dissolving lysozyme powder in water to approximately 80 mg/ml and acidifying to pH 3 with hydrochloric-acid stock solution. Gel-permeation chromatography was used to remove the ovalbumin and conalbumin contaminants from Sigma L-2879 lysozyme[19,20]. Lysozyme-rich eluate was concentrated to approximately 10 g/L *via* ultrafiltration through Diaflo YM10 membranes (Amicon; 10,000 g/mol MWCO) and dialyzed in

Spectrapor membrane tubing (Spectrum; 6-8,000 g/mol MWCO) against 50 volumes of potassium chloride solution of the desired ionic strength. Lysozyme concentration was determined by ultraviolet spectrophotometry using an extinction coefficient of $\varepsilon_{280\,nm}^{25°C} = 2.635$ L/(g-cm)[21]. Lysozyme concentration varied between 7 - 12 g/L (0.5 - 0.8 mmol/L); no effect of protein concentration on titration results was observed within this concentration range. Amino-acid solutions were prepared by dissolving into water the dry amino-acid powder and sufficient crystalline potassium chloride to prepare a solution of the desired ionic strength. Amino-acid concentrations were never greater than 5 mmol/L.

The exact concentrations of H^+ and OH^- in the acidic and alkaline titrant solutions were determined by first titrating the alkaline titrant against a standard solution containing a known amount of potassium hydrogen phthalate, then titrating the acidic titrant against a specified amount of the alkaline titrant. These titrant-concentration assays were performed at least in triplicate. A solution of 0.15% (v/v) phenolphthalein in ethanol was used as indicator.

3.4. Automated Titration Apparatus

Titration experiments were conducted in an airtight 100-mL, jacketed glass vessel sealed by a plexiglas lid with ports for titrant injection lines, gas lines, and the pH electrode. Vessel temperature was maintained at 25°C (±0.1°C) by recirculation of water through the vessel jacket and a thermostatted bath. The headspace was swept with argon at very small positive pressure during the titrations to remove airborne carbon dioxide. Argon was passed through a column packed with Drierite and acid-gas-specific molecular sieves to remove trace water and carbon dioxide, then resaturated by sparging through a gas-washing bottle filled with degassed, distilled, deionized water. Titrant aliquots of specified volume were injected through a fritted line by a Dosimat 665 precision pump (Metrohm; Westbury, NY). Solutions in the titration vessel were

agitated gently by a magnetic stirrer to speed pH equilibration after injection of each titrant aliquot. Hydrogen-ion activity was measured using a Ross combination semimicro electrode (Orion; Boston, MA), and the electrode response, E, was recorded by the control PC *via* an analog-to-digital converter board (Keithley Metrabyte DAS-1400; Cleveland, OH). Control software allowed automation of all experiments: titrant aliquots were injected until the pH endpoint was reached, with sufficient time for electrode equilibration between aliquot injections. Data in the form $\{E,V^{added}\}$ were saved for subsequent analysis. At any p°H value between 2.5 and 11.5, reproducibility between replicate titration curves was usually within 0.1 valence units; this variation was taken as the intrinsic uncertainty of the experimental method.

4. RESULTS

4.1. Experimental and Theoretical Protein Titration Curves

Figure 1 compares the titration curve for lysozyme in potassium-chloride solutions with other experimental results in the literature. The titration curve of Haynes *et al.*[22], shown in Figure 1(*a*), agrees with our measurements to within an average charge deviation of 0.3 units over the entire p°H range, with a maximum deviation of 0.8 charge units at p°H ~ 9.3. The older data of Tanford and Roxby[23] deviate significantly; these deviations may reflect the presence of protein impurities in their titrations. Similar agreement is shown in Figure 1(*b*) for the titration data reported here for solutions containing 0.2 M potassium chloride and the data of Sakakibara and Hamaguchi[24].

Figure 2(*a*) shows the experimental titration curve for hen-egg-white lysozyme measured in this work for solutions containing 0.1 M potassium chloride. Also shown in Figure 2(*a*) are two other titration curves for lysozyme calculated from the experimental pK_as of Kuramitsu and Hamaguchi

(solid line) and Beroza and Case (dotted line) listed in Table 1. Here, p°K_as were obtained from equation (3b), with γ_{H^+} calculated from Pitzer's model[18]. In these experiments lysozyme was dilute, and the assumption $\gamma_{HA_i} = \gamma_{A_i} = 1$ was made. There are two p°H regions in Figure 2(*a*) where the theoretical titration curve calculated from the pK_as computed by Beroza and Case differs sufficiently from our experimental curve (and from the curve calculated from the pK_as of Kuramitsu and Hamaguchi) to warrant discussion: the acidic region where p°H < 4 and the alkaline region where p°H > 11. For p°H < 4, the titrating groups are the side chains of the seven aspartic acid residues and Glu-7, and the C-terminal carboxyl group. A reasonable way to compare the differences between titration curves in this p°H region is to compare the average value of the aspartic-acid side-chain pK_a. Table 1 shows that the average value of the aspartic-acid side-chain pK_a is 2.9 for the results of Kuramitsu and Hamaguchi and 3.51 for the results of Beroza and Case. At a given p°H, titratable groups with higher pK_as remain more positively charged than groups with lower pK_as. Similarly, for p°H > 11, the theoretical titration curve of Beroza and Case is shifted by up to +1 charge unit relative to the curve calculated from the experimental pK_as of Kuramitsu and Hamaguchi because the theoretical side-chain pK_as of Tyr-20 and Tyr-23 are 1-2 pH units higher than the experimental values. Furthermore, in the limit of highest p°H, all titration curves should converge to $z_p = -13$. However, Beroza and Case assert pK_a = 16.89 for Tyr-53, an unrealistically high value, explaining why their titration curve remains offset by +1 charge unit from the two experimental titration curves as p°H increases to 14. If not for the unusually high pK_as computed for all three of lysozyme's tyrosyl side chains, the theoretical titration curve would be in excellent agreement with the experimental titration curves for p°H greater than 4.

As discussed above, any ΔpK_a is relative to some p$K_{a,\text{model}}$ that, in theory, reflects no electrostatic

interactions external to the titrating site itself. To obtain a simple experimental estimate of $pK_{a,model}$ for the titratable groups in lysozyme, free-amino-acid titrations were conducted in potassium chloride solutions for each of the amino acids bearing titratable groups found in lysozyme. Results from solutions with ionic strength 0.1 M are shown in Table 1; complete results for ionic strength to 3.0 M are given in Table 2. The side-chain pK_as measured in these titrations are not entirely free of the effect of intramolecular electrostatic interactions because for amino-acid monomers, the amino- and carboxy-terminal titratable groups are in relatively close molecular proximity to the side-chain titratable groups. More accurate estimates of the $pK_{a,model}$ values would in principle be obtained by titration of denatured proteins or end-blocked polypeptides. However, for the purpose of demonstrating the presence of pK_a perturbations in lysozyme, titration of monopeptides was considered sufficient.

Figure 2(*b*) shows all titration curves in Figure 2(*a*), with the addition of two new curves: one (dashed line) calculated from the $pK_{a,model}$ values measured from the free-amino-acid titrations conducted in 0.1 M potassium-chloride solutions; and one showing titration data (open squares) for denatured lysozyme in 6 M guanidine hydrochloride solution for p°H less than 7[23]. Good agreement of these two additional curves validates the choice of amino-acid monomers as model compounds for the acidic p°H region. The aspartic-acid side-chain $pK_{a,model}$ measured in free-aspartic-acid solution is 3.72, 0.8 pH unit higher than the average experimental pK_a of Kuramitsu and Hamaguchi. Consequently, because there are seven aspartic-acid residues in lysozyme, the titration curve calculated from the free-amino-acid $pK_{a,model}$ values (dashed line) shows a significantly higher net protein charge than either of the experimental lysozyme titration curves for p°H < 4. The theoretical titration curve calculated from the pK_as of Beroza and Case (shown in Figure 2(*b*) for p°H < 4 only) lies between the titration curve calculated from the free-amino-acid

p$K_{a,model}$s and the experimental curves, indicating that the electrostatic modeling efforts of Beroza and Case were partially successful in quantifying aspartic-acid side-chain ΔpK_as in lysozyme.

None of these authors investigated the hydrogen-ion equilibria of the eleven arginine side-chains in lysozyme. The pK_as of these groups are expected to be quite alkaline; the pK_a for the arginine side chain in the free-amino-acid titrations reported here is 12.77 in solutions with 0.1 M potassium-chloride concentration, well above the p°H range used in most titration experiments with lysozyme. In computing the pK_as of other titratable groups in the protein, Beroza and Case assumed that the arginine side chains are always protonated. Furthermore, the pK_a-regression technique of Kuramitsu and Hamaguchi was not sufficiently sensitive to extract eleven unique pK_as from such a narrow region of extreme p°H. It is reasonable to assume that the pK_as of these groups in the protein are perturbed, but the magnitudes of the perturbations have not yet been quantified. Therefore, in calculating the titration curves shown in Figure 2, the free-amino-acid value of arginine's side-chain pK_a was used as an approximation, in effect introducing eleven identical titratable groups with pK_a = 12.77.

Figure 3 shows experimental hydrogen-ion titration curves measured for lysozyme at 25°C in solutions where the potassium-chloride ionic strength varied from 0.1 to 2.0 M. Each curve represents an average of between two and seven titration experiments. At p°H = 2.5, the curves are well separated and show a trend of increasing net protein charge with increasing solution ionic strength. As p°H rises, the curves converge; for p°H > 5, the titration curves for ionic strength to 1.0 M all show net protein charges that agree to within 0.5 charge units. The titration curve for 2.0 M ionic strength differs: at p°H = 4.3, it crosses the 1.0 M curve and shows the lowest net protein charge of any titration curve for p°H between 5.2 and 9.1. Experimentally, the 2.0 M titration

solutions were not as stable as those with lower ionic strengths: for p°H greater than 9, protein macroaggregates were often observed in the titration vessel, and pH-electrode equilibration after each aliquot addition was less reliable. Hence, the 2.0 M data may not truly reflect the solution behavior of fully-solvated, non-aggregated lysozyme molecules, even in the acidic branch of the titration curve. While lysozyme is known to possess a monomer-dimer equilibrium at p°H above 5 in low-ionic-strength solutions[21], it was assumed not to affect the titration behavior of the protein.

All titration curves in Figure 3 are referenced to a common isoelectric point, p°I = 11.16, assumed constant with respect to ionic strength. The p°I would exhibit an ionic-strength dependence if the hydrogen-ion equilibria of titratable groups having pK_as near the p°I were dependent on ionic strength. In lysozyme, these groups are the six lysine residues. Table 2 shows that the p$K_{a,\mathrm{model}}$ value for lysine is 10.8 for ionic strengths 0.1 and 1.0 M. Further, the average lysine pK_as in Table 1, both those regressed by Kuramitsu and Hamaguchi and those calculated by Beroza and Case, agree with p$K_{a,\mathrm{model}}$ to within 0.5 p°H units at 0.1 M ionic strength. Hence the isoelectric point of lysozyme is assumed not to depend on ionic strength.

4.2. Lysozyme Surface-Charge Interactions

Rasmol molecular-graphics visualization of hen-egg-white lysozyme (Brookhaven PDB structure 2LYZ) shows that most titratable groups reside on or near the molecular surface. Therefore, in the extreme acidic limit, the surface of lysozyme is highly positively charged. As the p°H increases, the low-pK_a groups (*i.e.*, the aspartic-acid and glutamic-acid side chains) deprotonate and become negatively charged, interacting favorably with the positively charged lysine and arginine residues. The presence of the positively charged lysine and arginine groups on the surface favors

deprotonation of the acidic residues, reflected as negative pK_a perturbations for these residues. Table 1 shows that the experimental ΔpK_a is, on average, –0.8 pH units for the aspartic acid residues and -1.6 pH units for Glu-7, relative to the $pK_{a,model}$ values measured for free amino acids in 0.1 M potassium chloride solution. (The *positive* pK_a perturbation of Glu-35 has been explained above.) These negative ΔpK_a perturbations produce the downward shift in the experimental titration curve, relative to the curve calculated from the $pK_{a,model}$ values, observed in Figure 2(*b*).

As ionic strength increases, electrostatic interactions between solvent-accessible surface residues diminish due to dielectric screening. Therefore, addition of mobile salt ions to the protein solution reduces the magnitude of the negative pK_a perturbations of the acidic groups, giving pK_as that increase with rising ionic strength, as verified experimentally by Abe, *et al.*[10]. These authors used two-dimensional NMR methods to probe the effect of ionic strength on the hydrogen-ion equilibria of the acidic residues of hen-egg-white and turkey-egg-white lysozymes, over a range of salt concentrations from 5 to 400 mM, in sodium chloride solutions. Hence, for the acidic residues, as the ionic strength increases, dielectric screening of surface electrostatic interactions also increases; negative pK_as perturbations relax; and the titration curves shift upward to show a higher net protein charge at any given p°H, as shown in Figure 3. Similarly, for any p°H above the isoelectric point, the protein has a net negative charge and pK_a perturbations increase the protein's net charge; in general, these are positive pK_a perturbations for the alkaline titratable groups. As ionic strength increases at high p°H, screening of surface electrostatic interactions decreases the positive pK_a perturbations and the titration curve shifts downward. On a plot such as Figure 3, these ionic-strength-dependent pK_a shifts produce a clockwise rotation of the titration curve around the isoelectric point as ionic strength increases. This rotation phenomenon has been previously

reported for other soluble globular proteins where most of the titratable residues are surface-accessible[25,26]. However, it is not readily observed in Figure 3 because lysozyme's isoelectric point is so high.

4.3. Ion Binding to Lysozyme

Lysozyme is known to bind chloride ions in a manner that depends on both the solution pH and ionic strength[27]. To construct comprehensive molecular descriptions of protein-salt interactions in aqueous salt solutions, especially at ionic strengths where salt-induced phase equilibria occur, it is necessary to have experimental information about the extent of ion binding by protein. Fraaije and Lyklema[1,7,8] have developed a general molecular-thermodynamic description of ion binding that requires knowledge of the ionic-strength dependence of hydrogen-ion titration curves. These authors have applied this model to predict binding of chloride ions to bovine serum albumin[1]. The central principle of this theory is that the binding number, r_i, of any dissolved species i is related to the binding numbers of all other species. Hence, hydrogen-ion-binding information contained in protein-titration data is required to obtain (in our case) potassium-ion and chloride-ion binding numbers. The binding number for chloride ion, for example, depends on both ionic strength and p°H and is expressed in terms of the protein charge by:

$$r_{Cl^-} = \frac{z_p}{2} - \frac{1}{2} \cdot \int_{\mathrm{pI}}^{\mathrm{p^\circ H}} \delta_{a/b} d\mathrm{p^\circ H} \qquad (6)$$

where the Esin-Markov coefficient $\delta_{a/b}$ is defined as:

$$\delta_{a/b} \equiv \left(\frac{\partial z_p}{\partial \log a_s} \right)_{\mathrm{p^\circ H}, c_p} \tag{7}$$

and incorporates the ionic-strength dependence of the protein-titration data. The salt activity, $a_s = m\gamma^{\pm}$, where m is the salt molality and $\gamma^{\pm}$ is the mean-ionic activity coefficient, obtained here from Pitzer's model[18]. The potassium binding number is calculated from the overall electroneutrality relation for the protein molecule plus its surrounding dielectric double layer:

$$r_{K^+} = r_{Cl^-} - z_p \tag{8}$$

In the context of this general model, ion "binding" refers to preferential interaction of ions with the protein, relative to the bulk solution, either by binding tightly to the protein or by associating loosely in the diffuse double layer.

The protein net charge, z_p, was obtained as a function of p°H and ionic strength from the lysozyme titration curves of Figure 3. Multivariable regression was used to fit the titration data to the p°H and ionic-strength axes simultaneously. Calculations were implemented using MathCad Professional 7.0 software. Coefficients $\delta_{a/b}$ were obtained by establishing a fit of z_p to $\log a_s$ at each p°H, for ionic strength to 1.0 M. The 2.0 M titration curve was not included in the $\delta_{a/b}$ calculations because it behaves in a manner inconsistent with the trend of the lower-ionic-strength curves, as discussed above. Coefficients $\delta_{a/b}$ are shown in Figure 4 as a function of p°H for ionic strength 0.1 M. The lysozyme titration curves show the greatest ionic-strength dependence for

p°H less than 5; consequently, this p°H region is where the values of $\delta_{a/b}$ are largest. For p°I < p°H < 11.35 (the upper p°H limit in these calculations), $\delta_{a/b}$ in Figure 4 has a small negative value as a result of the inversion of the ionic-strength dependence of the lysozyme titration curves at p°H above the isoelectric point.

Figures 5(*a*) and 5(*b*) show, respectively, binding numbers for chloride ions and potassium ions to lysozyme, calculated from equation (8). These numbers reflect preferential interaction of the ions with lysozyme, relative to their concentrations in the reference solution (the lysozyme-free salt solution). Chloride binding is highest at low p°H, where the protein is most positively charged and counter-ions partition preferentially into the diffuse double layer. At p°H above the isoelectric point, where lysozyme bears a negative net charge, slight "negative" binding occurs. This corresponds to expulsion of chloride anion, now a co-ion, from the double layer. The ionic strength dependence of chloride binding is greatest at low p°H where the protein is highly charged. As ionic strength rises, the net charge of the protein increases, as shown in Figure 3; consequently, more counter-ions selectively partition into the diffuse double layer. As p°H increases toward the isoelectric point, the dependence of the protein net charge on ionic strength decreases, as previously discussed, and therefore, the ion-binding numbers also depend less on ionic strength. Figure 5(*b*) shows that potassium-ion binding exhibits trends with p°H and ionic strength opposite to those of chloride ion, as determined by the requirement of overall electroneutrality of the protein molecule plus double layer.

5. CONCLUSION

Hydrogen-ion titrations of hen-egg-white lysozyme were conducted over the p°H range 2.5 to 11.5, with ionic strength to 2.0 M. These data provided two kinds of information useful for molecular-thermodynamic description of protein-solution behavior. First, the function z_p allows direct evaluation of net protein charge over a wide range of solution pH and ionic strength. An independent measure of the protein net charge reduces the experimental effort in regression of other adjustable parameters in any model for describing thermodynamic properties of protein solutions. Second, binding numbers for chloride and potassium ions were obtained from the ionic-strength dependence of the hydrogen-ion titration curves. As modern trends in molecular-thermodynamic models move toward incorporating salt ions as discrete species in solution, physicochemical data will be required to quantify interactions between salt ions and proteins; ion-binding numbers provide such information. For example, the multicomponent adhesive-hard-sphere model, used previously to describe ion clustering[5,28], relates binding numbers to intermolecular potential parameters. Also, titrations were conducted for eleven of the twenty natural L-amino acids in potassium-chloride solutions at ionic strengths to 3.0 M. Measured pK_as of N-terminal, C-terminal, and side-chain hydrogen-ion equilibria are reported. Because we have not found any amino-acid pK_as in the literature for ionic strengths greater than 1.0 M, the data given here provide significant additions to the existing base of knowledge of amino-acid acid/base equilibria in electrolyte solutions.

Amino-Acid Residue	Exptl. pK_a Ref. K&H[17]	Calculated pK_a Ref. B&K[12]	Calculated pK_a Ref. B&C[14]
N-term (Lys)	7.9	5.0	7.27
Asp-18	2.0	2.6	3.00
Asp-48	4.3	1.6	3.33
Asp-52	3.4	8.5	5.66
Asp-66	1.6	2.2	2.69
Asp-87	2.1	0.8	3.15
Asp-101	4.5	4.3	3.37
Asp-119	2.5	1.3	3.35
Asp average	*2.9*	*3.8*	*3.51*
Glu-7	2.6	1.2	2.60
Glu-35	6.1	6.2	4.69
His-15	5.8	2.4	6.71
Lys-1	10.8	10.8	10.57
Lys-13	10.5	10.1	10.75
Lys-33	10.6	7.7	9.94
Lys-96	10.8	8.9	9.82
Lys-97	10.3	8.4	10.51
Lys-116	10.4	9.7	10.22
Lys average	*10.6*	*9.3*	*10.30*
Tyr-20	10.3	12.1	12.00
Tyr-23	9.8	10.1	10.89
Tyr-53	12.1	18.8	16.89
C-term (Leu)	3.1	2.2	3.10

Amino-Acid Titrations (0.1M KCl)
N-term: 9.21
Asp: 3.72
Glu: 4.17
His: 6.06
Tyr: 10.17
Lys: 10.81
Arg: 12.77
C-term: 2.32

Table 1: pK_a values for titratable groups in hen-egg-white lysozyme, from various authors, and from free-amino-acid titrations.

Amino Acid	I = 0.1M C-term pK_a	N-term pK_a	Side pK_a	I = 1.0M C-term pK_a	N-term pK_a	Side pK_a	I = 3.0M C-term pK_a	N-term pK_a	Side pK_a
Alanine	2.36	9.86	–	2.44	9.76	–	2.72	10.10	--
Arginine	2.08	9.09	12.77	2.27	9.28	12.87	2.55	9.63	12.83
Asparagine	2.18	8.73	–	2.28	8.83	–	2.46	9.13	--
Aspartic Acid	2.00	9.72	3.72	2.05	9.58	3.68	2.26	9.89	3.94
Cysteine	1.95	10.36	8.23	2.01	10.26	8.24	2.27	10.39	8.44
Glutamic Acid	2.22	9.64	4.17	2.18	9.49	4.11	2.50	9.74	4.43
Histidine	1.71	9.15	6.06	1.94	9.18	6.26	2.15	9.45	6.60
Isoleucine	2.33	9.64	–	2.43	9.72	–	2.71	10.04	--
Leucine	2.32	9.64	–	2.43	9.75	–	2.70	10.01	--
Lysine	2.10	9.21	10.81	2.29	9.39	10.85	2.62	9.70	11.01
Tyrosine	2.22	9.04	10.17	2.33	9.09	10.02	2.62	9.36	10.18

Table 2: Amino-acid carboxy-terminal, amino-terminal, and side-chain pK_as measured in solutions of potassium chloride with ionic strength 0.1 M, 1.0 M, and 3.0 M, at 25°C. Arginyl side-chain pK_as were obtained by extrapolation of the titration curve past the upper p°H endpoint (usually approximately 12.5).

NOTATION

a_i	activity of species i
c_i	molar concentration of species i
E	electrode voltage response
E^{ref}	electrode reference potential
I	ionic strength
$K_{a,i}$	hydrogen-ion dissociation equilibrium constant of titratable group i
m_i	molal concentration of species i
r_i	binding number of species i
S	electrode slope
z_p, z_i	net charge of protein, species i

Greek Symbols

γ_i	single-ion activity coefficient of ionic species i
$\gamma^{\pm}$	mean-ionic activity coefficient
$\delta_{a/b}$	Esin-Markov coefficient

FIGURE CAPTIONS

Figure 1: Experimental hydrogen-ion titration curves for hen-egg-white lysozyme in solutions of potassium chloride at ionic strength: (a) 0.1 M; and (b) 0.2 M.

Figure 2(*a*): Experimental and theoretical titration curves for hen-egg-white lysozyme in 0.1 M potassium chloride solutions.

Figure 2(*b*): Experimental and theoretical titration curves for hen-egg-white lysozyme in 0.1 M potassium chloride solutions.

Figure 3: Dependence of experimental titration curves on solution ionic strength, for hen-egg-white lysozyme in potassium chloride solutions.

Figure 4: Dependence of Esin-Markov coefficient on p°H for hen-egg-white lysozyme in 0.1 M potassium chloride solutions.

Figure 5(*a*): Chloride-ion binding numbers in solutions of hen-egg-white lysozyme and potassium chloride.

Figure 5(*b*): Potassium-ion binding numbers in solutions of hen-egg-white lysozyme and potassium chloride.

LITERATURE CITED

(1) Fraaije, J. G. E. M.; Lyklema, J. *Biophys. Chem.* **1991a**, *39*, 31-44.

(2) Kuehner, D. E.; Blanch, H. W.; Prausnitz, J. M. *Fluid Phase Equil.* **1996**, *116*, 140-147.

(3) Kuehner, D. E.; Heyer, C.; Rämsch, C.; Fornefeld, U. M.; Blanch, H. W.; Prausnitz, J. M. *Biophys. J.* **1997**, *73*, 3211-3224.

(4) Vlachy, V.; Blanch, H. W.; Prausnitz, J. M. *AIChE J.* **1993**, *39*, 215-223.

(5) Chiew, Y. C.; Kuehner, D. E.; Blanch, H. W.; Prausnitz, J. M. *AIChE J.* **1995**, *41*, 2150-2159.

(6) Coen, C. J.; Blanch, H. W.; Prausnitz, J. M. *AIChE J.* **1995**, *41*, 996-1004.

(7) Fraaije, J. G. E. M.; Murris, R. M.; Norde, W.; Lyklema, J. *Biophys. Chem.* **1991b**, *40*, 303-315.

(8) Fraaije, J. G. E. M.; Norde, W.; Lyklema, J. *Biophys. Chem.* **1991c**, *40*, 317-327.

(9) Bartik, K.; Redfield, C.; Dobson, C. M. *Biophys. J.* **1994**, *66*, 1180-1184.

(10) Abe, Y.; Ueda, T.; Iwashita, H.; Hashimoto, Y.; Motoshima, H.; Tanaka, Y.; Imoto, T. *J. Biochem.* **1995**, *118*, 946-952.

(11) Spassov, V.; Karshikov, A.; Atanasov, B. *Biochim. Biophys. Acta* **1989**, *999*, 1-6.

(12) Bashford, D.; Karplus, M. *Biochem.* **1990**, *29*, 10219-10225.

(13) Bashford, D.; Karplus, M. *J. Phys. Chem.* **1991**, *95*, 9556-9561.

(14) Beroza, P.; Case, D. A. *J. Phys. Chem.* **1996**, *100*, 20156-20163.

(15) You, T. J.; Bashford, D. *Biophys. J.* **1995**, *69*, 1721-1733.

(16) Gibas, C.; Subramaniam, S. *Biophys. J.* **1996**, *71*, 138-147.

(17) Kuramitsu, S.; Hamaguchi, K. *J. Biochem.* **1980**, *87*, 1215-1219.

(18) Pitzer, K. S. *Activity Coefficients in Electrolyte Solutions*, 2nd ed.; CRC Press: Boca Raton, 1991.

(19) Lorber, B.; Skouri, M.; Munch, J.-P.; Giegé, R. *J. Cryst. Growth* **1993**, *128*, 1203-

1211.

(20) Skouri, M.; Lorber, B.; GiegÈ, R.; Munch, J.-P.; Candau, J. S. *J. Cryst. Growth* **1995**, *152*, 209-220.

(21) Sophianopoulos, A. J.; Van Holde, K. E. *J. Biol. Chem.* **1964**, *239*, 2516-2524.

(22) Haynes, C. A.; Sliwinsky, E.; Norde, W. *J. Coll. Interf. Sci.* **1994**, *164*, 394-409.

(23) Tanford, C.; Roxby, R. *Biochem.* **1972**, *11*, 2192-2198.

(24) Sakakibara, R.; Hamaguchi, K. *J. Biochem.* **1968**, *64*, 613-618.

(25) Luo, C. Protein Charge and Ion Binding in High Ionic Strength Electrolyte Solutions. M.S., University of California, Berkeley, 1997.

(26) Edsall, J. T. Proteins as Acids and Bases. In *Proteins, Amino Acids, and Peptides*; Cohn, E. J., Edsall, J. T., Eds.; Reinhold: New York, 1943.

(27) Carr, C. *Arch. Biochem. Biophys.* **1953**, *46*, 417-423.

(28) Barboy, B.; Tenne, R. *Chem. Phys.* **1979**, *38*, 369.

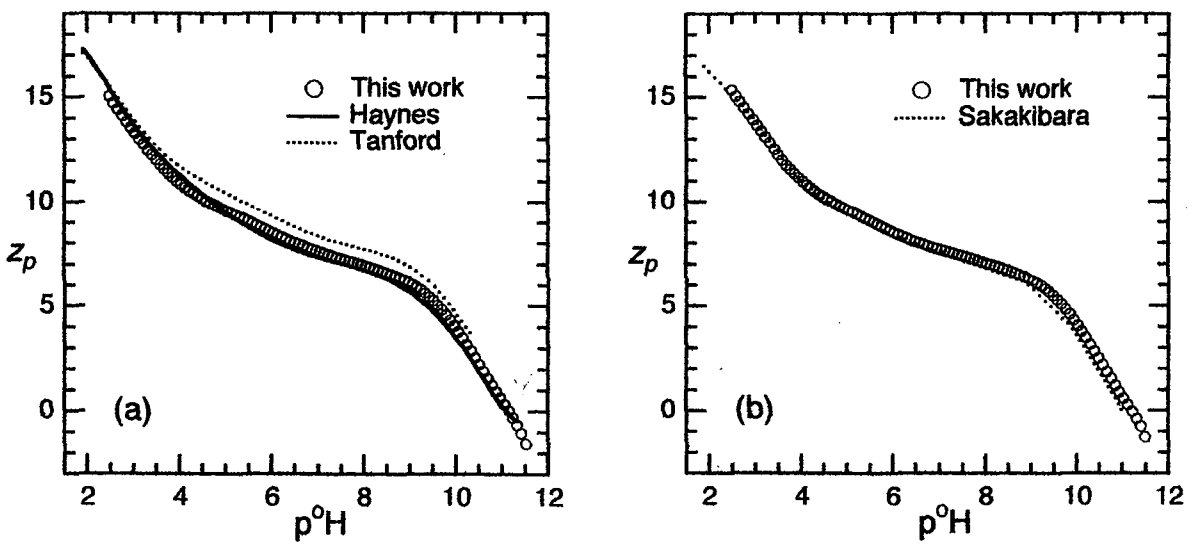

Figure 1
Kuehner, et al.

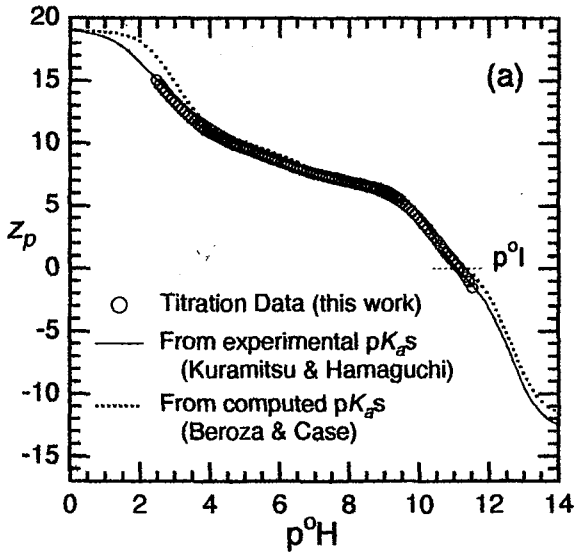

Figure 2(*a*)
Kuehner, et al.

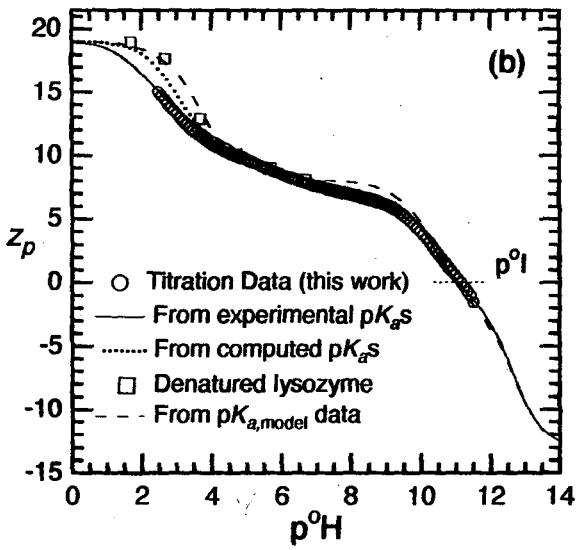

Figure 2(*b*)
Kuehner, et al.

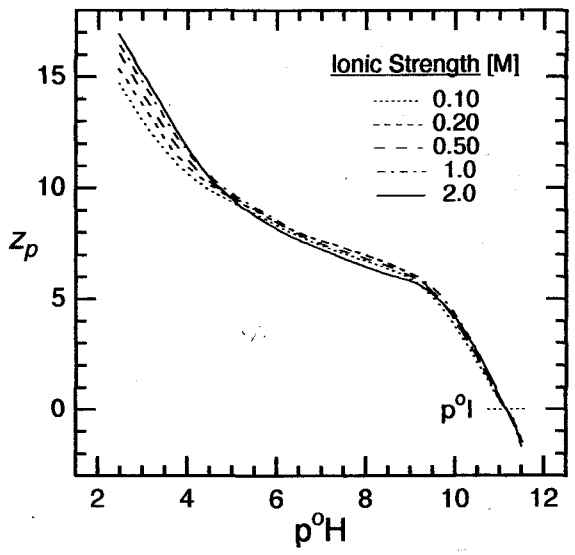

Figure 3
Kuehner, et al.

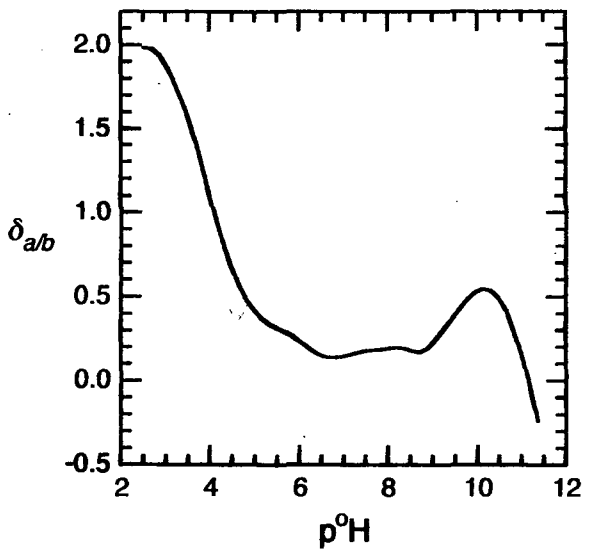

Figure 4
Kuehner, et al.

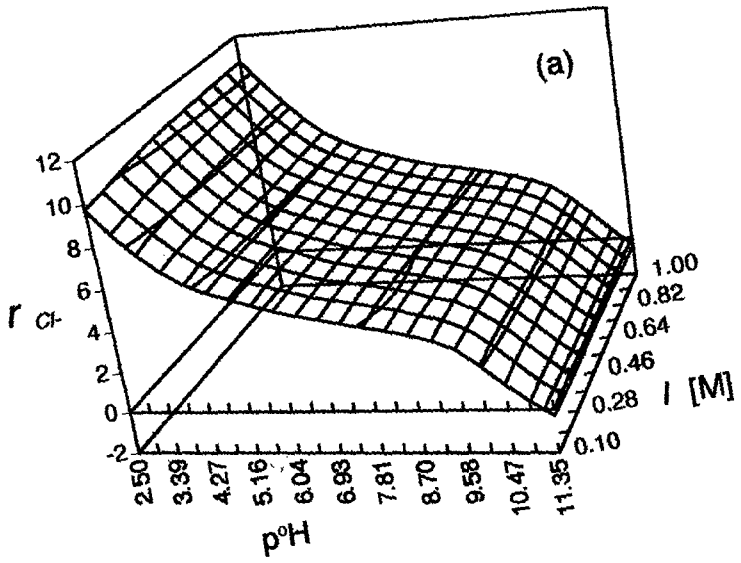

Figure 5(*a*)
Kuehner, et al.

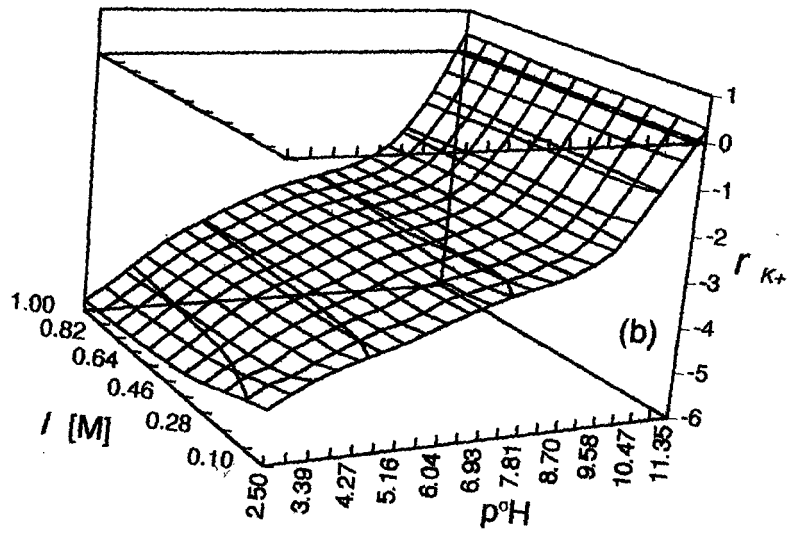

Figure 5(*b*)
Kuehner, et al.

Ernest Orlando Lawrence Berkeley National Laboratory
One Cyclotron Road | Berkeley, California 94720

Prepared for the U.S. Department of Energy under Contract No. DE-AC03-76SF00098